Improving temporal resolution of surrogate model for nuclear accident prediction with SRCNN

Taeyeon Min [a], Semin Joo [a], Yeonha Lee [a], Seok Ho Song [a], Jeong Ik Lee [a*]
[a]*Department of Nuclear and Quantum Engineering, Korea Advanced Institute of Science and Technology; 373-1 Guseong-dong Yuseong-gu, Daejeon 305-701, Republic of Korea*
[*] *Correspinding author: jeongiklee@kaist.ac.kr*

Keywords: SRCNN, surrogate model, time-resolution, peak detection, severe accident

1. Introduction

The progression of a severe accident in a nuclear power plant is highly complex, characterized by non-linear dependencies on various thermal-hydraulic (TH) and physical variables, necessitating significant computational resources for confident prediction. Consequently, artificial intelligence (AI) is increasingly being employed for predicting severe accidents in nuclear power plants [1]. Once fully trained, AI has the potential to significantly lower the computational costs, enabling its use as an Accident Management Support Tool (AMST) to aid operators in decision-making during accidents, thereby minimizing the risk of human error. The methodology of accident prediction using AI is mainly based on surrogate models that learn from data produced by existing severe accident simulation codes.

The authors' research team applied DNNs to develop a supervised learning-based surrogate model for accident prediction [2]. The accident scenario is total-loss-of-component-cooling-water (TLOCCW) in OPR1000, and the length of the time series is 72 hours, which is considered in Probabilistic Safety Assessment. The model employed the rolling window forecasting method to simulate the accident's progression, revealing that as the number of time steps increased (corresponding to higher time resolution), the accumulated error also increased. The previous study found that the accumulated error of time series data according to the time step of 1 hour, 30 minutes, and 15 minutes was checked [3]. In the case of the surrogate model with 15 minutes interval, the error tends to increase compared to 1 hour interval model. This finding suggests that accident predictions with a time resolution higher than 1 hour cannot guarantee the reliability of the surrogate model due to excessive error accumulation. Consequently, a method is required to convert low-resolution (LR) data into high-resolution (HR) data without significant data loss. To address this issue, this paper proposes a high-resolution accident prediction model using SRCNN, a deep learning model originally designed for high-resolution image restoration [4].

.

2. Methods

2.1 Selection of accident scenario

The accident scenario for training the AI model is the total loss of component cooling water (TLOCCW), which was previously selected by the previous studies. A TLOCCW accident is a failure of all seven safety-related components of a reactor. (See Table I.) In generating the TLOCCW accident scenario, the following failures of safety components were assumed: the RCP seal LOCA has an 89.2% chance of failure within the first hour. Failures of the HPI, LPI, CSS, and charging pump are tied to the depletion of the refueling water storage tank (RWST), which is depleted between 7 and 8 hours in over 80% of cases, leading to failures during this period. Other component failures were assumed to occur randomly.

Table I. List of components that fail at TLOCCW

Reactor coolant pump (RCP) seal LOCA
Letdown heat exchanger (HX)
High-pressure (HPI) injection pump
Low-pressure (LPI) injection pump
Containment spray system (CSS) pump
Motor-driven auxiliary feedwater (MDAFW) pump
Charging pump

In addition, three severe accident management guidelines (SAMGs) were randomly initiated within 72 hours. SAMG is a set of protocols developed to guide operators in managing and mitigating the consequences of severe accidents. If a monitored variable meets a certain condition, the corresponding SAMG strategy is activated. The three SAMGs employed in this study are SG injection (M1), RCS depressurization (M2), and RCS injection (M3).

2.2 Data production

To generate the accident scenario, MAAP 5.03 code was used. The MAAP code calculated the progression of severe accident over a 72-hour period and returns various TH variables. The target TH variables were selected as 10 variables monitored in the main control room (MCR) (see Table II). Therefore, a single accident scenario consists of time series data of 10 TH variables from 0 to 72 hours after the accident occurred. The total dataset is composed 11,000 TLOCCW accident scenarios.

Table II. List of target TH variables

Primary system pressure
Hot leg temperature
Cold leg temperature
Reactor vessel water level (RV WL)
Steam generator pressure (SG P)

Steam generator water level (SG WL)
Maximum core exit temperature (Max CET)
Containment pressure (CTMT P)
Pressurizer pressure (PZR P)
Pressurizer water level (PZR WL)

The datasets were normalized to values between 0 and 1, which is necessary for transforming the time series to two dimensional images with Gramian Angular Summation Field (GASF). Moreover, datasets were extracted with 60, 30, 15, and 10-minute intervals for training the SRCNN model.

2.3 Imaging and restoring time series: GASF

Imaging time series is necessary because the required input and output dataset for SRCNN are two-dimensional matrix. Moreover, converted 2D datasets should recover into 1D. The transformation and restoration are utilized GASF [5]. The GASF is a representation of time series data as an image in a non-Cartesian coordinate system. GASF has two steps to convert time series data to a matrix.

Given the time series $X = \{x_1, x_2, \dots, x_n\}$, after normalization to [0,1] the rescaled time series $\tilde{X}$ preserve the one-to-one correspondence through the angular transformation (see Eq. (1)).

$$\begin{cases} \phi_i = \arccos(\tilde{x_i}), 0 \le \tilde{x_i} \le 1, \ \tilde{x_i} \in \tilde{X} \\ r = \frac{t_i}{N}, t_i \in N \end{cases} \quad Eq.(1)$$

where t_i is the stamp and N is a constant factor to regularize the span of the polar coordinate system.

GASF is obtained as the sum of the angles of polarized time series data at time points i and j (see Eq. (2, 3)).

$$GASF = \left[\cos(\phi_i + \phi_j)\right] \quad Eq.(2)$$

$$= \tilde{X}' \cdot \tilde{X} - \sqrt{I - \tilde{X}^2}' \cdot \sqrt{I - \tilde{X}^2} \quad Eq.(3)$$

where I is the unit row vector $[1,1,\dots,1]$.

Since the GASF matrix is not dependent on the value of r, it is also not affected by the value of L used to transform the time series into polar coordinates. The diagonal elements of a GASF are equal to $\cos(2\phi_i)$, and interval of ϕ_i is $\left[0, \frac{\pi}{2}\right]$. Therefore, diagonal elements are a one-to-one correspondence in interval of transformed angle, this allows restoration to a one-dimensional time series without significant loss.

The performance of the transformation and restoration is evaluated by root mean square error (RMSE) (see Eq. (4)). RMSE is the quadratic mean of the differences between the time series obtained MAAP code and applying transformation and restoration for each TH variables. The thermodynamic variable with the largest RMSE is PZR WL, which is negligible at 10^{-12}.

$$RMSE = \sqrt{\frac{1}{N}\sum_{i=1}^{N} \left| y_{GASF,i} - y_{MAAP,i} \right|^2} \quad Eq.(4)$$

where N is the number of data in one scenario, $y_{GASF,i}$ is time series applied transformation and restoration from $y_{MAAP,i}$ by using GASF, and $y_{MAAP,i}$ is time series predicted by MAAP.

2.4 Structure of the SRCNN model

The SRCNN framework employed in this study comprises two stages (see Figure 1.). The first stage involves preprocessing, where a one-dimensional time series is transformed into a two-dimensional image, followed by upsampling the low-resolution time series or matrix. The time series is upsampled using linear interpolation, while the matrix is upsampled using bilinear interpolation. As a result, the preprocessing stage is categorized into two sequences that involve data upsampling and conversion, designated as 'UC' and 'CU'. The second stage is the super-resolution (SR) process, which consists of three convolutional layers. The initial convolutional layer applies a relatively small kernel (9x9) to extract features from small patches of the upsampled image. These extracted features are then passed through the second convolutional layer, which uses a medium-sized kernel (1x1) to perform a non-linear transformation. Finally, the third convolutional layer, with a small kernel (5x5), merges the non-linearly transformed feature maps to reconstruct the final high-resolution image.

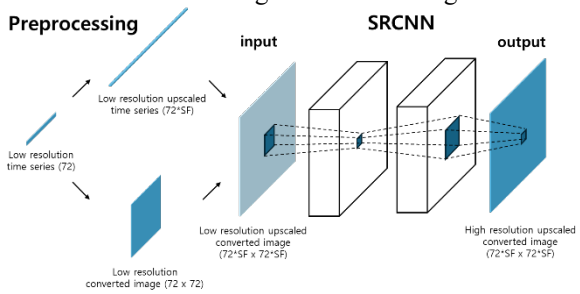

Fig. 1 The overall framework of SRCNN consists of two stages.

The input data consists of LR time series of one of the 10 TH variables, sampled with 1-hour intervals for 72-time steps, extracted using the MAAP code. In the preprocessing stage, this time series is converted and upsampled into LR images (matrices) with 30, 15, and 10-minute intervals. The SRCNN model then reconstructs these LR matrices into HR matrices, maintaining the same number of time steps as the original LR matrices. Consequently, 10 SRCNN models, one for each TH variable, are trained for SR at scale factors of 2, 4, and 6. The datasets are divided into training, validation, and test sets with 8:1:1 ratio.

The performance of the models is evaluated using two different metrics: mean square error (MSE) and peak signal-to-noise ratio (PSNR). PSNR is a widely used metric for assessing the quality of a reconstructed or compressed image compared to its original version. It quantifies the difference between the original and reconstructed images, providing a measure of the fidelity of the reconstructed image. PSNR is defined using the MSE between the original and reconstructed images.

The hyperparameters for the SRCNN framework were configured as follows: the preprocessing

transformation processes 'UC' and 'CU', and the configuration of number of CNN filters: (64/32/1), (128/64/1), (256/128/1). Optimization was conducted across these six combinations. The results indicated that for all three scale factors, the 'UC' transformation process with the filter configuration (64/32/1) demonstrated the best performance (see Table IV).

Table IV. Error metrics of SRCNN model for best performance case

Time intervals	**30min**		**15min**		**10min**	
error metrics	MSE	PSNR	MSE	PSNR	MSE	PSNR
(64/32/1) UC	0.00581	37.09	0.00729	34.90	0.00732	33.503

2.5 Structure of the surrogate model

To validate the SRCNN model's ability to predict high-resolution scenarios without loss, the authors compared the time series predicted by applying SRCNN to a surrogate model generated with 1-hour intervals with the high-resolution time series predicted by the surrogate model. The surrogate model was employed Long Short-Term Memory (LSTM) (see Fig 2.)

The input layer is composed of 10 TH variables, 7 component failure times, and 3 SAMG activation times at the previous 3-time steps. The hidden layer is optimized into 400 nodes and 32 batch size in previous study [6]. Consequently, 10 surrogate models, one for each TH variable, are trained. As a result, the 1100 scenarios of each TH variables were generated same with test set of SRCNN model.

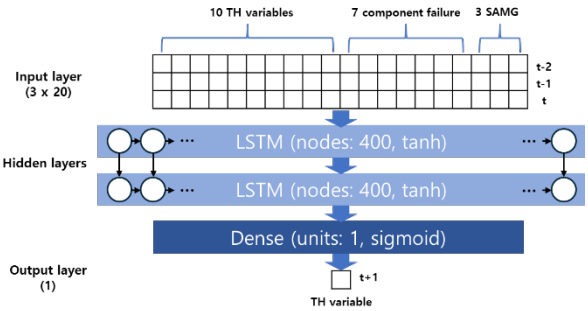

Fig. 2. The overall framework of surrogate model.

3. Results

To validate the SRCNN model's ability to predict high-resolution scenarios without loss, the authors compared the time series predicted by applying SRCNN to a surrogate model generated at 1-hour intervals with the time series predicted by the surrogate model. These are based on difference with 1-minute intervals MAAP time series.

3.1 Comparison of DTW distance

First, the dynamic time warping (DTW) distance was employed. The DTW distance is an algorithm that measure the similarity between two sequences that vary in time, a popular way to show the similarity between two time series of data. The normalized mean DTW distance are compared in Fig. 3 for various time intervals and DNN models.

When comparing the DTW distance between the original MAAP data and the predictions for all TH variables, it was generally observed that the time series generated using the surrogate model and those generated with SRCNN (applied to the time series created at one-hour intervals) exhibited a decreasing DTW distance as the time resolution increased.

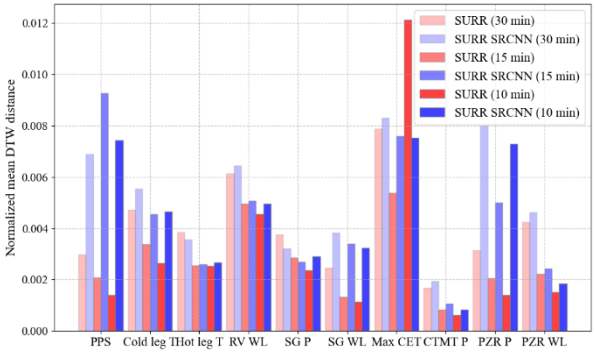

Fig.3. Normalized mean DTW distances of TH variables of surrogate model and SRCNN model.

3.2 Comparison of Peak time

Next, the authors compared the peaks in the time series predicted by the MAAP code with those predicted by two AI models to evaluate their ability to preserve the peaks in the predicted data. Accurately predicting the timing of peaks in TH variables during a severe accident is crucial, as these peaks represent the moments closest to reactor failure and provide the least margin for safety.

To detect these peaks, a characterization peak function $S(i, x_i, T)$ was defined. A point x_i in the time series $T = \{x_1, x_2, \dots, x_n\}$ is considered a peak if it satisfies specific conditions defined by $S(i, x_i, T)$. This function calculates the average of the maximum signed distances of x_i from its k left neighbors and the maximum signed distances of x_i from its k right neighbors (see Eq. (5)). The value of $S(i, x_i, T)$ indicates the significance of x_i relative to its neighboring values [7].

$$S(i, x_i, T) = \frac{max(x_i - x_{i-1}, \dots, x_i - x_{i-k}) + max(x_i - x_{i+1}, \dots, x_i - x_{i+k})}{2}$$
$$if\ i > k\ and\ i \leq N - k \qquad Eq\ (5)$$

The pseudo-code for detecting the peaks from a times series data is shown below.

Algorithm peak detection
Input *T / time series data*
k / window size around the peak
h / significance multiplier
Output
P / selected peaks
Start
$P = \emptyset$;
for (i = 1; i < N; i ++) **do**
$s(i) = S(i, x_i, T)$;
end for

Compute the mean μ and standard deviation σ of all positive values in s;
for ($i = 1; i < N; i ++$) **do**
if $(s(i) > 0 \;\&\&\; s(i) - \mu \geq h * \sigma)$ **then** $P = P \cup x_i$
end if
end for
for each adjacent pairs of peaks x_i, x_j *in P,* **do**
if $|i - j| \leq k$ **then**
remove smaller value of the pair from P
end if
end for
end start

In the peak detection method, the parameter h was set to 1.7. Given the various time steps in the time series data, the parameter k was adjusted to maintain a consistent 1-hour interval (for 10-minute interval, k was set to 6). This adjustment was determined through a process of trial and error.

Next, if the difference between the time points of the peak detected in the MAAP time series and the time point of the peak detected in the time series predicted by the two DNN models is smaller than the time step of the DNN model, it was assumed to be true positive detection. The peak detection was evaluated using two performance metrics: true positive rate (TPR) and precision. The TPR indicates the proportion of actual positive cases that the model correctly identifies. Precision measures the proportion of cases predicted as positive that are indeed positive, reflecting the accuracy of the model's positive predictions.

$$TPR = \frac{TP}{TP + FN} \qquad Eq\ (6)$$

$$Precision = \frac{TP}{TP + FP} \qquad Eq\ (7)$$

where TP, FN and FP stand for true positive, false negative and false positive, respectively. Table V shows the performance metrics of each TH variable in the test data for various time intervals and DNN models

Table V. Performance metrics of peak detection of TH variable: TPR (top) and Precision (bottom)

Time interval	30 minutes		15 minutes		10 minutes	
DNN model	Surrogate model	SRCNN	Surrogate model	SRCNN	Surrogate model	SRCNN
PPS	0.504	0.539	0.517	0.411	0.559	0.413
Hot leg T	0.642	0.610	0.647	0.605	0.639	0.579
Cold leg T	0.642	0.658	0.641	0.588	0.610	0.451
RV WL	0.538	0.534	0.490	0.495	0.445	0.178
SG P	0.383	**0.807**	0.151	**0.541**	0.461	**0.539**
SG WL	0.183	0.176	0.548	0.152	0.559	0.142
Max CET	0.494	0.474	0.442	0.401	0.438	0.374
CTMT P	0.923	0.830	0.930	0.463	0.929	0.517
PZR P	0.506	**0.546**	0.338	0.235	0.332	**0.371**
PZR WL	0.615	**0.647**	0.656	0.638	0.668	0.648

Time interval	30 minutes		15 minutes		10 minutes	
DNN model	Surrogate model	SRCNN	Surrogate model	SRCNN	Surrogate model	SRCNN
PPS	0.933	0.740	0.907	0.481	0.761	0.441
Hot leg T	0.843	0.801	0.688	0.538	0.741	0.553
Cold leg T	0.943	0.779	0.868	0.696	0.811	0.422
RV WL	0.367	**0.726**	0.286	**0.306**	0.356	0.139
SG P	0.509	**0.955**	0.207	**0.596**	0.596	0.554
SG WL	0.205	0.197	0.623	0.148	0.660	0.127
Max CET	0.437	0.380	0.399	0.315	0.421	0.390
CTMT P	0.871	**0.875**	0.867	0.470	0.854	0.496
PZR P	0.964	0.723	0.604	0.236	0.544	0.391
PZR WL	0.920	**0.934**	0.892	0.826	0.869	0.837

4. Conclusions and Further Works

In this study a methodology is developed to improve the temporal resolution of accelerated predictions for severe nuclear power plant accidents using an SRCNN model. By comparing the performance of the SRCNN model with a surrogate model across different time intervals, while SRCNN offers competitive performance in certain scenarios, the surrogate model generally outperformed SRCNN, particularly in terms of accurately capturing critical peak.

Since the SRCNN model predicts by smoothing the data, it is characterized by a sharp decrease in DTW and peak preservation metrics for TH variables that are highly oscillatory, such as SG WL, as the time interval of the predicted time series decreases. In the case of peak preservation, there were thermodynamic variables for which the performance metrics increased. However, in general, the performance metrics was lower than the surrogate model when the upscaling was larger, such as 10 minutes. These findings suggest that while SRCNN has potential as a method for enhancing data resolution, further optimization is necessary for it to be fully effective in real-time, high-stakes applications such as nuclear power plant accident management.

Acknowledgements

This work was supported by KOREA HYDRO & NUCLEAR POWER CO., LTD (No. 2020-Tech-01).

REFERENCES

[1] Na, M. G. *et al*. Prediction of major transient scenarios for severe accidents of nuclear power plants, *IEEE Transactions on Nuclear Science*, *51*(2), 313–321, 2004

[2] Lee, Y. *et al*. Applications of Neural Network to Predict Reactor Vessel Failure Time for Various Component Failures during Severe Accident, *Transactions of the Korean Nuclear Society Spring Meeting, Jeju*, 2022

[3] Joo, S. *et al*. Accelerated prediction of severe accident progression: Sensitivity of deep neural network performance to time resolution, *Transactions of the Korean Nuclear Society Autumn Meeting, Gyeongju, 2023*.

[4] Dong, C. *et al*. *Image Super-Resolution Using Deep Convolutional Networks*. http://arxiv.org/abs/1501.00092, 2014.

[5] Wang, Z. *et al*. *Imaging Time-Series to Improve Classification and Imputation*. http://arxiv.org/abs/1506.00327, 2015.

[6] Joo, S. Development of an Explainable Machine Learning Methodology for Accelerated Prediction of Nuclear Power Plant Severe Accident Scenario, Master's thesis, KAIST, 2024.

[7] Palshikar, Girish. Simple algorithms for peak detection in time-series. Proc. 1st Int. Conf. advanced data analysis, business analytics and intelligence. Vol. 122. 2009.